

LIQUID AND SOLID ION PLASMAS

D.J. Wineland, Wayne M. Itano, J.C. Bergquist, S.L. Gilbert,
J.J. Bollinger, and F. Ascarunz

National Bureau of Standards, Boulder, CO 80303

ABSTRACT

Experiments on strongly-coupled nonneutral ion plasmas, performed at the National Bureau of Standards, are summarized. We first discuss strong coupling of small numbers (< 100) of macroscopic and atomic ions confined in Paul (electrodynamic) traps, in which crystalline structures are observed. We then discuss experiments in which shell structure is observed for up to 10^4 atomic ions confined in static electric and magnetic fields. In our experiments, we have progressed from working with very small numbers of ions up to an intermediate value. Future experiments are suggested, including some where infinite volume behavior might be observable.

INTRODUCTION

This paper briefly summarizes the work on strong coupling in nonneutral ion plasmas at the National Bureau of Standards at Boulder. This work has grown out of a project whose goal is very high resolution atomic spectroscopy on samples of ions contained in an "ion trap." Since spectral lines are, in general, shifted and broadened by Doppler effects associated with the motion of the ions, we desire an accurate characterization of the velocity distributions of the nonneutral plasmas (or "clouds") of ions contained in these traps.

Our interest in the strong coupling problem was in part stimulated by a 1977 paper¹ of Malmberg and O'Neil who discussed the possibility of achieving liquid and solid like behavior of a pure electron nonneutral plasma confined by static electric and magnetic fields. Their confinement device has typically been called a Penning trap² by atomic physicists. At about this time, we demonstrated the method of laser cooling³ on atomic ions in a Penning trap.⁴ Since the achievable temperatures are in the millikelvin range and below, we realized that strong coupling could probably be achieved in such a sample of ions. In addition, at low temperatures, the resonant light scattering cross section for atomic ions can be on the order of 10^{-10} cm². This is to be compared to the Thomson cross-section for electrons which is approximately 10^{-24} cm². Therefore, for atomic ions, the large cross sections for light scattering and long confinement times (many hours) made it possible to take pictures and "movies" of the plasmas. This sensitivity is dramatically illustrated by the pictures of single ions.^{3,5,6}

The static thermodynamic properties of an ion cloud confined in a trap are identical to those of a one-component plasma (OCP).^{1,7} An OCP consists of a single species of charged

particles embedded in a uniform-density background of opposite charge. For the system of ions in a trap, the trapping fields play the role of the neutralizing background charge. An OCP can be characterized by the Coulomb coupling constant,^{1,7}

$$\Gamma \equiv q^2 / (a_s k_B T), \quad (1)$$

which is a measure of the nearest neighbor Coulomb energy divided by the thermal energy of a particle. The quantities q and T are the ion charge and temperature. The Wigner-Seitz radius a_s is defined by $4\pi a_s^3 n_0 / 3 = 1$, where $-qn_0$ is the charge density of the neutralizing background. An infinite volume OCP has been predicted⁷ to exhibit liquid-like behavior (short range order) for $\Gamma > 2$ and a liquid-solid phase transition to a bcc lattice at $\Gamma \approx 178$.

The occurrence of spatial ordering when $\Gamma > 1$ can be understood qualitatively. At low enough temperature, where $\Gamma > 1$, the ions do not have enough kinetic energy to overcome the Coulomb repulsion. Therefore they cannot approach each other very closely and become more evenly spaced. Even though this basic idea is understood, interest in this subject has continued to grow, possibly due to the richness of phenomena expected⁷ and the difficulty of achieving this condition experimentally. Moreover, strong coupling has been studied or is expected in many fields besides plasma physics, for example in: 2-D configurations of electrons or ions near the surface of liquid helium,^{8,9} charged particles in liquid suspension which act through a shielded Coulomb potential,¹⁰ electrons in solids (Wigner crystallization), astrophysics (Curtis Michel, this conference) and perhaps somewhat surprisingly, in particles which are confined in high energy storage rings and cooled by electron cooling.¹¹

ION TRAPS

Atomic physicists have most often used two kinds of devices in ion trapping work, the Penning trap and the Paul (radio-frequency) trap² whose electrodes are shown schematically in Fig. 1. The Penning trap is essentially the same device as that used in other nonneutral plasma studies.^{12,13} In atomic physics experiments, the electrodes are often made to conform to equipotentials of a quadratic potential (Fig. 1). This insures that motion of single ions (or the center-of-mass motion for a single species) is harmonic. Thus the "hyperbolic" traps can be used as charge-to-mass analyzers. Ions in a Penning trap can be thought of as comprising an OCP where the static magnetic and electric fields play the role of the neutralizing background charge.^{1,13}

The Paul (rf) trap typically uses the same electrode configuration as shown in Fig. 1. Trapping is provided by the ponderomotive potential or pseudopotential, resulting from the application of spatially inhomogeneous, time varying electric

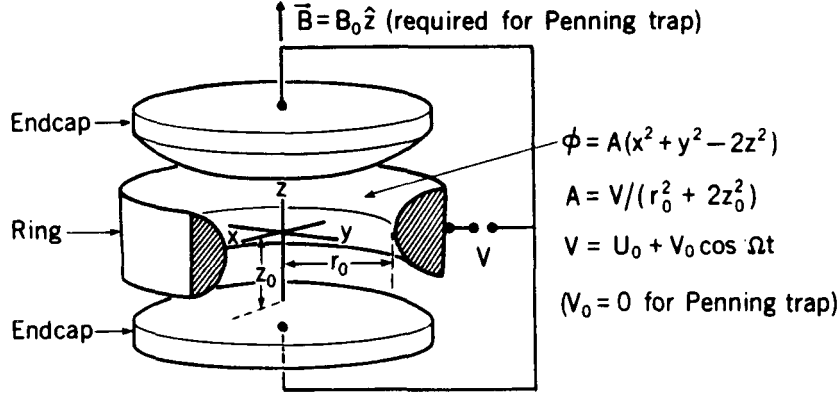


Fig. 1 Schematic representation (cutaway view) of the electrode configuration for the Paul (rf) or Penning trap. Electrode surfaces are figures of revolution about the z axis and are equipotentials of $\phi(r,z)=A(r^2-2z^2)$. For this equation, cylindrical coordinates are used with the origin at the center of the trap. Typical dimensions are $\sqrt{2}z_0 = r_0 \approx 1$ cm. Typical operating parameters are the following: for the Paul trap, $V_0=300$ V, $\Omega/2\pi \approx 1$ MHz; for the Penning trap, $U_0=1$ V, $B=1$ T.

fields.² For the hyperbolic trap (Fig. 1) this ponderomotive potential takes the form^{2,14}

$$\phi_p = \alpha r^2 + \beta z^2, \quad (2)$$

where

$$\alpha = qV_0^2 / (m\Omega^2 \xi^4) + U_0 / \xi^2 \quad (3a)$$

$$\beta = 4qV_0^2 / (m\Omega^2 \xi^4) - 2U_0 / \xi^2. \quad (3b)$$

$\xi^2 = r_0^2 + 2z_0^2$, m is the ion mass, and the other parameters are defined in Fig. 1. The center-of-mass oscillation frequencies of ions in the quadratic potential of Eq. 2 are usually called the secular frequencies.²

Equation 2 is equivalent to the potential inside of a uniformly charged spheroid.¹⁴ Therefore, ions confined in a Paul trap may be thought of as comprising an OCP where the uniform neutralizing background charge density has the shape of a uniformly charged spheroid consistent with Eq. 2. This picture is valid when the micromotion of the ions at the drive frequency Ω can be neglected. For large numbers of ions this is not always justified as discussed below.

The Penning and Paul traps can be superimposed; the general solution was given by Fischer.¹⁵ OCP properties have been discussed in Ref. 14.

MACROSCOPIC PARTICLE PAUL TRAP EXPERIMENTS

The Paul trap was experimentally demonstrated in 1959.¹⁵ In the experiments of Wuerker, et al., macroscopic aluminum particles (diameter $\approx 20 \mu\text{m}$) were stored. The charges on these particles were quite high ($\approx 5 \times 10^5$ electron charges) leading to $\Gamma \gg 1$ and the observation of regular crystalline arrays. The key to these experiments is the high value of q . Since $\Gamma \propto q^2$, large values of Γ can be obtained even though the interparticle spacings are macroscopic ($\sim 1 \text{ mm}$) and temperatures were near room temperature.



Fig. 2. Cluster of alumina particles (center part of picture) in a Paul trap. Endcaps are not visible in this picture; inner diameter of ring electrode is 2.5 cm, $\Omega/2\pi = 60 \text{ Hz}$.

We have performed experiments similar to those of Ref. 15. In Fig. 2, we show a suspension of approximately 25 alumina particles (clumps of grinding powder) which have crystallized into a regular array. The inner part of the ring electrode (diameter $\approx 2.5 \text{ cm}$) is visible but the endcap electrodes are obscured from view. For this picture, we had $V_0 \approx 350 \text{ V}$ at $\Omega/2\pi = 60 \text{ Hz}$. Although the electrode surfaces were not hyperbolic, their shapes were chosen by computer calculation¹⁶ to make the potential near the center of the trap nearly quadratic. The dimensions of an equivalent hyperbolic trap are $r_0 = 1.36 \text{ cm} = \sqrt{2} z_0$. The background gas pressure for this trap was about 13 Pa (100 mTorr) of air which maintained the particle temperature near 300 K. From either the measured secular frequency along the z axis of symmetry, or from the potential applied to one endcap in order to counteract gravity (the z axis is vertical) we determined that the charge-to-mass ratio is $q/m \approx 10^{-10} \times q/m(\text{proton})$. From the

separation of two charged particles in the x-y plane ($U_0 = 0$), we determined that the mass of the particles was approximately 10^{-9} g and therefore the particle's charge was about $q = 6 \times 10^4 \times q(\text{proton})$. (For $U_0 = 0$, the balance of the pseudo potential (inward) force by the Coulomb repulsion (outward) is charge independent, but mass dependent). This gives a value of $\Gamma \gtrsim 10^5$. For Fig. 2, the particles were illuminated by a laser but a simple lamp would suffice.

MACROSCOPIC VS. ATOMIC PARTICLE EXPERIMENTS

Under fairly simple experimental conditions, very high values of Γ can be obtained in the macroscopic particle experiments because of the high values of charge obtained. It is therefore reasonable to ask why we would like to use atomic ions where the charge is much smaller, typically $q = q(\text{proton})$. One reason is that for a given size of the ion sample with respect to the trap dimensions, the number of ions N_1 is proportional to q^{-1} (see Appendix A). Therefore, if we desire samples of many particles, small charge on the particles is advantageous. Perhaps more important is that in the macroscopic particle experiments, q and m are difficult to control precisely so that comparison of the observed crystals with theory is more difficult to make. Also, even though the macroscopic particles have high charge, their mass is relatively high and their charge-to-mass ratio q/m relatively small compared to atomic particles (typically about 10 orders of magnitude smaller). This consideration is important for Penning trap confinement where the maximum density given by the Brillouin density¹⁷ is equal to $n_{\text{max}} = B^2/(8\pi mc^2)$. For the macroscopic particles of Fig. 2, we estimate $m = 10^{-9}$ g, so that even for $B = 10$ T, $n_{\text{max}} \approx 4 \times 10^{-4}$ cm⁻³ which is extremely small (not to mention the problems with stray electric fields). For atomic particles, $n_{\text{max}} \approx 10^{10}$ cm⁻³. Thus, magnetic confinement of large numbers of particles can only be accomplished with atomic or molecular ions or electrons. Finally, atomic ions have internal structure which can be spectroscopically probed to give information on plasma dynamics.¹⁸ Therefore, even though the macroscopic particle traps can provide interesting information on the strong coupling problem, many experiments require atomic ions or electrons.

STRONGLY COUPLED ATOMIC IONS IN PAUL TRAPS

With the practical density and charge limitations imposed on atomic ions in Penning and Paul traps, very low temperatures must be realized in order to obtain $\Gamma \gg 1$. This has been achieved by laser cooling.³ Here we describe an experiment using Hg^+ ions at NBS.¹⁸ A similar experiment has been performed at the Max Planck Institute for Quantum Optics in Garching.¹⁹

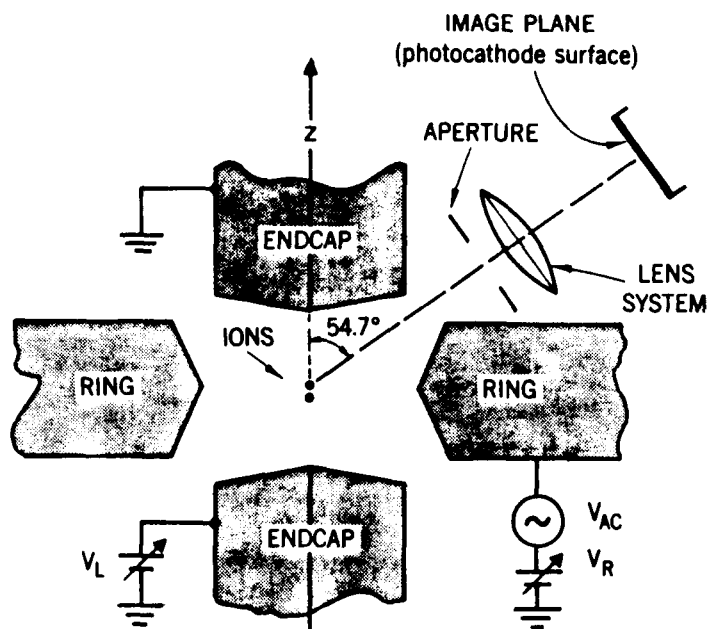


Fig. 3 Schematic drawing of the trap electrodes (to scale) and imaging system (not to scale) for Hg^+ cluster experiments. The end-cap to end-cap separation along the z axis is approximately $625 \mu\text{m}$. The overall magnification of the lens system is 180X. The laser beam used to illuminate the ions also enters the trap at an angle of 54.7° with respect to the z axis and is perpendicular to the observation axis shown.

Small numbers of $^{198}\text{Hg}^+$ ions were stored in a miniature Paul trap, which has properties equivalent¹⁶ to those of a hyperbolic trap with dimensions $r_0 \approx 466 \mu\text{m}$ and $z_0 \approx 330 \mu\text{m}$. An oscillating voltage V_0 with peak amplitude between 145 and 325 V at a frequency of 23.26 MHz was applied between the ring and end-cap electrodes for trapping. The ions were laser cooled by 1-2 μW of cw 194-nm radiation²⁰ (bandwidth < 2 MHz), whose beam waist was varied between 5 and 15 μm at the position of the ions. This radiation was tuned near the $5d^{10}6s^2S_{1/2} \rightarrow 5d^{10}6p^2P_{1/2}$ first resonance line, which has a natural linewidth of 70 MHz. Some of the 194-nm fluorescence from the ions was focused onto the photocathode of a resistive-anode photon-counting imaging tube as shown schematically in Fig. 3. The optics for this imaging was provided by a three-stage fused-quartz lens system with an aberration-compensated first stage. The first lens was apertured to give an f number of 4.5. The positions of the photons detected by the imaging tube could be displayed on an oscilloscope in real time or stored by a computer in order to make time exposures.

In Fig. 4(a) we show the orientation of the trap as viewed by the imaging tube. In Fig. 4(b), two ions are made to lie in the x-y plane by making $\alpha < \beta$ in Eq. 2. Although the trap was designed to have axial symmetry, the preferred spatial alignment of the two cold ions indicates that an asymmetric potential exists which could be due to trap imperfections, contact-potential variations, or some other trap asymmetry. For convenience, we choose this preferred direction to be the x axis as indicated in Fig. 4b.

In the remainder of Fig. 4 we show images obtained for a few cases of up to 16 ions. We can characterize the ponderomotive potential as in Eqs. 2 and 3 or, equivalently, by the single ion resonance frequencies ν_z and ν_r for the motion in the axial and radial directions respectively. (In Fig. 4, we assume $\nu_x \approx \nu_y = \nu_r$.) We chose this latter method in Ref. 18 and for Fig. 4 since the measured oscillation frequencies²¹ are a more direct means of characterizing the trap than the applied potentials and trap dimensions. We find $\alpha = 2\pi^2 m\nu_r^2/q$ and $\beta = 2\pi^2 m\nu_z^2/q$ where α and β are from Eq. 2. When ν_z/ν_r is made large enough, all of the ions are forced by the strength of the potential in the z direction to lie in the x-y plane as in Figs. 4b and d. When ν_z/ν_r is small enough, the ions lie along the z axis as in Fig. 4c. This allowed us to count the ions. Below the images in Figs. 4d through 4g, we show the configurations obtained theoretically²² for each value of the number of ions N_i obtained by minimizing the function

$$E_\phi = q \sum_{i=1}^{N_i} (\alpha r_i^2 + \beta z_i^2) + q^2 \sum_{i < j}^{N_i} |\vec{r}_i - \vec{r}_j|^{-1} \quad (4)$$

where α and β are determined from the experimentally measured values of ν_r and ν_z .

The circular images or rings in Figs. 4e through g are due to ion circulation about the z axis. For a small asymmetry in the x,y plane, we can modify Eq. 2 to be approximately

$$\phi_p = \alpha_x x^2 + \alpha_y y^2 + \beta z^2. \quad (5)$$

When $\alpha_x < \alpha_y < \alpha_z$, and $N_i = 2$, the potential energy of Eq. 4 is minimized for two ions along the x axis as in Fig. 4b. The strength of this alignment is given by ΔE_ϕ , the maximum variation of E_ϕ for 2 ions constrained in the x-y plane. This is given by the difference between E_ϕ for ions on the x axis and E_ϕ for ions constrained along the y axis. For 3 or more ions in the same ring, the maximum variation in E_ϕ is considerably smaller than for two ions. Therefore, the ions more easily rotate in the azimuthal direction even though they must be nominally equally spaced in the ring. The number of ions in Fig. 4e could be

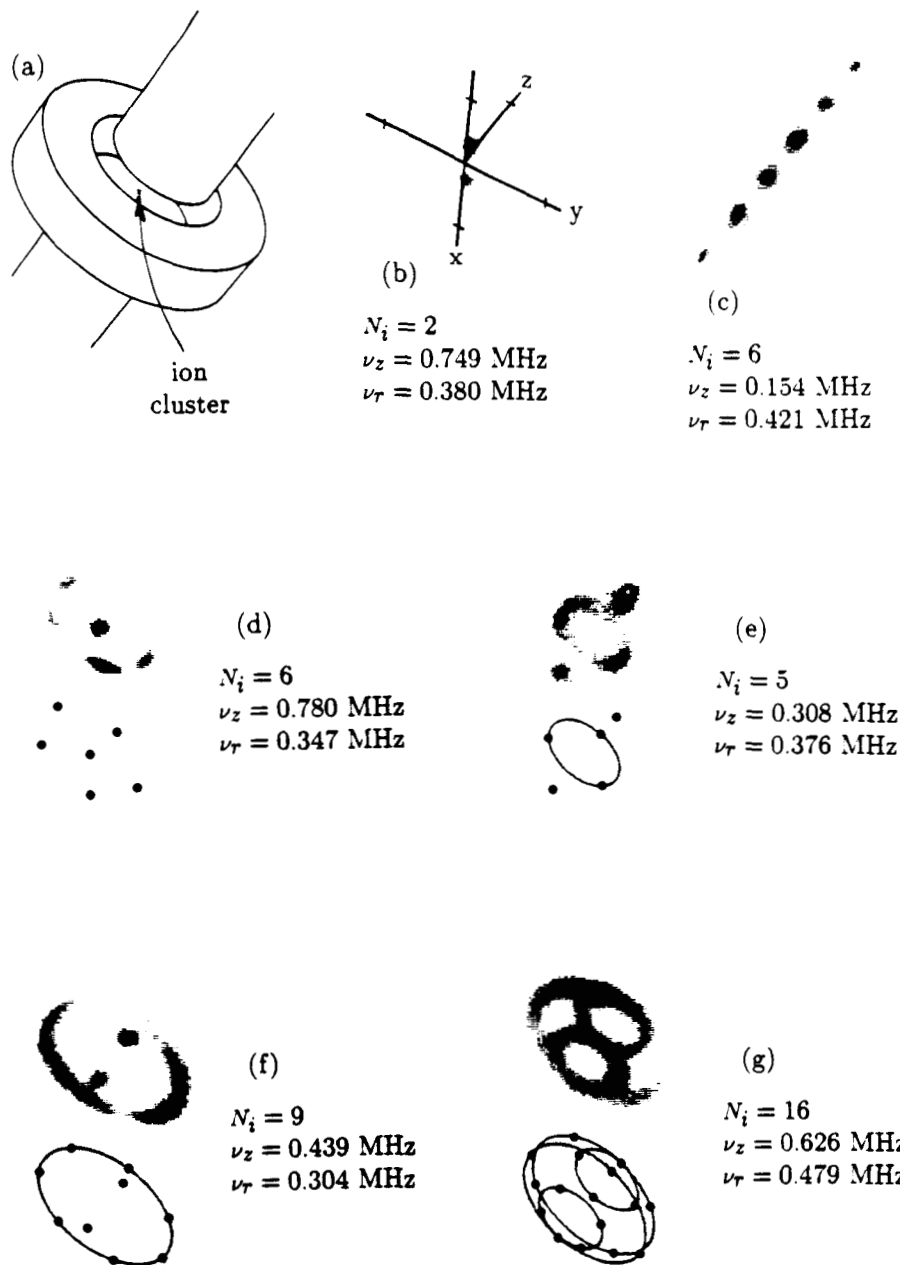
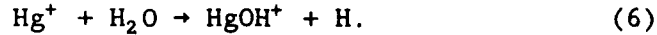


Fig. 4 Images of Hg^+ ion "clusters" in a Paul trap. In (a), the trap electrodes are shown schematically in the same orientation as for the remainder of the pictures, but at reduced magnification (inner diameter of the ring electrode is ≈ 0.9 mm). The coordinate system in (b) applies to the rest of the images. The tick marks on the axes are $10 \mu\text{m}$ from the origin. In (d) through (g), we display numerical solutions for the expected cluster shapes using the experimental values of ν_z and ν_r . The "rings" are caused by ion circulation about the trap z axis of symmetry. In (d), a non-fluorescing impurity ion occupies a particular ion site in the cluster and helps to pin the ions in the radial plane.

verified by aligning them along the z axis and counting. For Figs. 4f and g, the number of ions could be assigned by varying ν_z/ν_r and comparing the observed images (with rings) with the simulations. In principle, we could have aligned and counted 9 and 16 ions along z, but the ratio ν_z/ν_r required to do this was so low, that ions would have evaporated from the trap along the z axis.

In Fig. 4d, we see the approximate configuration expected for 6 ions but one of the ions appears to be missing. In addition, the ions are pinned in the x-y plane rather than forming a ring as in Fig. 4f. These observations are consistent with a nonfluorescing or "phantom" ion that occupies the missing cluster site. This ion may be another isotope of Hg^+ . For example, fluorescence from $^{199}\text{Hg}^+$ would be extremely weak because of ground state hyperfine optical pumping. It might also be an impurity molecular ion like HgOH^+ formed from the exothermic reaction



In any case, an impurity ion with charge-to-mass ratio different from $^{198}\text{Hg}^+$ will make ΔE_ϕ for ions in the same ring be larger than ΔE_ϕ if all the ions are $^{198}\text{Hg}^+$. This can happen because of the differences in α and β for ions of different charge-to-mass ratio. Thus we would expect pinning to be more likely with the impurity ion present. In the experiments of Ref. 19, the trap asymmetry in the x-y plane was probably larger than observed here. This apparently made ΔE_ϕ larger for ions in the same ring, resulting in pinning of like ions.

For these configurations, the agreement between data and simulations appears to be fairly good.²² To estimate Γ , we use for the background density n_0 the expression¹⁴

$$n_0 = \frac{1}{2\pi q} (2\alpha + \beta) = \frac{\pi m}{q^2} (2\nu_r^2 + \nu_z^2) \quad (7)$$

For the conditions of Fig. 4(g), Eq. 7 implies $n_0 = 3.8 \times 10^9$.

In these experiments, the temperature was extracted from the Doppler broadening of the ion's spectral lines.²³ This broadening contributes significantly to the width of $^2S_{1/2} \rightarrow ^2D_{5/2}$ quadrupole transition in $^{198}\text{Hg}^+$.^{18, 24} From these measurements, we determined that the secular motion temperature for two ions in the trap, when $\nu_r \approx 2\nu_z = 473$ kHz, was less than 8 mK. If we take 8 mK as a typical upper limit for the ions in fig. 4g then we obtain $\Gamma \geq 525$.

Finally, in Fig. 4g, we see that 16 ions approximately lie on 3 rings. The larger ring, containing 8 ions, lies in the x-y plane and the smaller rings, each containing 4 ions, lie in planes above and below but parallel to the x-y plane. We may also view these ions as lying on the surface of a spheroidal

shell characteristic of the structure for large numbers of ions.^{11, 13, 26-28}

In principle, it should be possible to observe ordered structures of much larger numbers of atomic ions in Paul traps. In our trap, this was apparently prevented for $N_1 \gtrsim 20$ because the small amount of laser power available for cooling was unable to overcome the rf heating.²⁵ In rf heating, the kinetic energy of the ion's driven motion at frequency Ω is coupled into the secular motion characteristic of the pseudopotential well.

STRONGLY COUPLED ATOMIC IONS IN PENNING TRAPS

In Penning traps,² where ions are confined by static electric and magnetic fields, rf heating²⁵ does not take place and large collections of ions can be laser-cooled to temperatures less than 10 mK. The static properties of ions in a Penning trap are identical to those of a one component plasma where the background density is given by^{1, 13, 14}

$$n_0 = \frac{m\omega}{2\pi q^2}(\Omega_c - \omega) . \quad (8)$$

Here, Ω_c is the ion cyclotron frequency and ω is the rotation frequency of the cloud. For a finite plasma consisting of a hundred to a few thousand ions, the boundary conditions are predicted to have a significant effect on the plasma state. Several molecular dynamics simulations on collections of a hundred to a few thousand ions confined in storage rings and traps have recently been completed.^{11, 26-28, 30, 31} When $\Gamma > 1$, the ions are predicted to reside in concentric shells. As the ions are cooled, instead of a sharp phase transition, the system is expected to gradually evolve from a liquid state characterized by short range order and diffusion in all directions, to a state where there is diffusion within a shell but no diffusion between the shells (like a smectic liquid crystal) and ultimately to an overall solid-like state.²⁸

We have investigated²⁹ this interesting system using ${}^9\text{Be}^+$ ions trapped in the cylindrical Penning trap shown schematically in Fig. 5. A magnetic field $\vec{B} = B\hat{z}$ ($B = 1.92$ T) produced by a superconducting magnet confined the ions in the direction perpendicular to the z axis. A static potential U_0 between the end and central cylinders confined the ions in the z direction to a region near the center of the trap.

The ${}^9\text{Be}^+$ ions were laser cooled by driving the $2s \ ^2S_{1/2} (m_I = 3/2, m_J = 1/2) \rightarrow 2p \ ^2P_{3/2} (3/2, 3/2)$ transition slightly below the resonant frequency. The 313 nm cooling radiation ($\approx 30 \ \mu\text{W}$) could be directed perpendicular to the magnetic field and/or along a diagonal as indicated in Fig. 5. In addition to cooling the ions, the laser also applied an overall torque which could either compress or expand the cloud.^{14, 23} This allowed us to control the cloud size by choosing the radial positions (and thus the torques) of the perpendicular and diagonal beams.

About 0.04% of the 313 nm fluorescence from the decay of the $^2P_{3/2}$ state was focused by f/10 optics onto the photocathode of the same imaging tube used in the Hg^+ ion experiments. The imager was located along the z axis, about 1 m from the ions. The imaging optics was composed of a three stage lens system with overall magnification of 27 and a resolution (FWHM) of about 5 μm . Positions of the photons arriving at the imager were displayed in real time on an oscilloscope while being integrated by a computer.

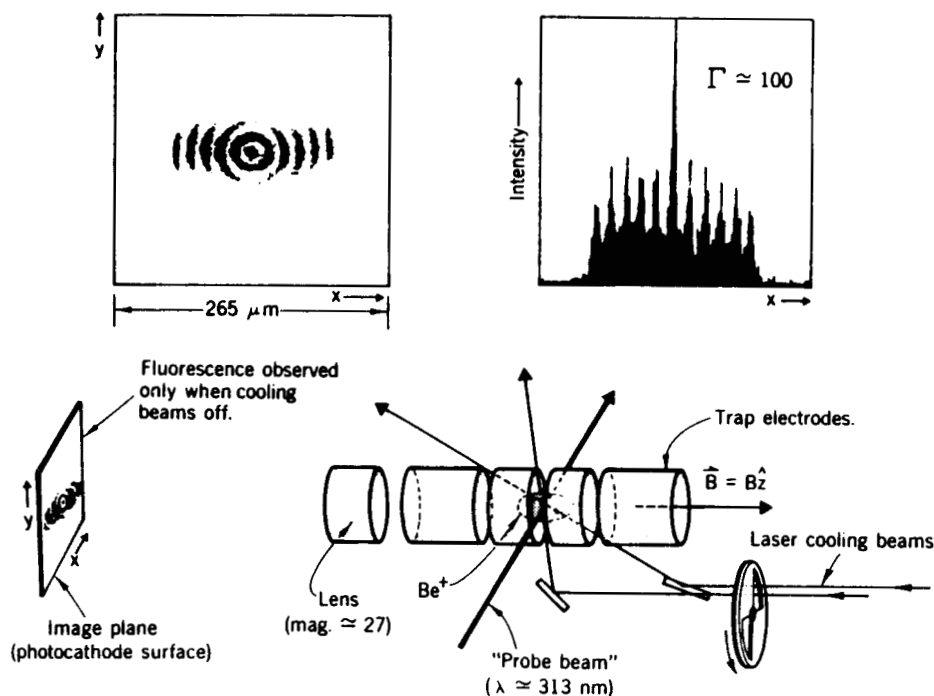


Fig. 5. Schematic representation of apparatus for observation of shell structure of strongly coupled $^9Be^+$ ions in a Penning trap. Images are made of the ions which are intersected by the probe beam. In the upper right, an intensity plot vs x for a value of y intersecting the center of the cloud is shown. Shell structure results from the boundary conditions at the edge of the cloud.

A second laser (power $\approx 1 \mu W$, beam waist $\approx 30 \mu m$) was used to spatially map the shell structure of the cloud. This probe laser was tuned to the same transition as the cooling laser and was directed through the cloud perpendicularly to the magnetic field. With the probe laser on continuously, the cooling laser could be chopped at 1 kHz (50% duty cycle) and the image signal integrated only when the cooling laser was off as shown in Fig. 5. Different portions of the cloud could be imaged by translating the probe beam, in a calibrated fashion, either parallel or perpendicular to the z axis. Images were also obtained from the ion fluorescence of all three laser beams.²⁹

The rotation frequency ω was determined from the first order Doppler shift of the ion's optical spectrum due to the cloud

rotation.^{23,29,32} From ω and an independent measurement of Ω_c ,²¹ n_0 was determined from Eq. 8. From the Doppler broadening of the spectrum, T was determined.^{23,29,32} From n_0 and size of the ion cloud, N_1 was determined. Γ was determined from n_0 and T .

We have observed clouds containing from 1 shell ($N_1 \approx 20$) up to 16 shells ($N_1 \approx 15\,000$). For a spherical cloud, approximately $(N_1/4)^{1/3}$ shells are predicted.²⁶ For the nearly spherical cloud of Ref. 29 ($N_1 \approx 15\,000$) this formula predicts 15.5 shells and we measured 16. At present, it is difficult to make further quantitative comparisons between our data and the theoretical calculations. For example, there is substantial uncertainty in our measurement of Γ due to uncertainty in the temperature measurement. Also, the spatial resolution is partially limited by optics. Our data do agree qualitatively with the simulations with the exception of the presence, in some cases, of an open cylinder shell structure²⁹ as opposed to the predicted closed spheroids. Schiffer has suggested³⁰ that shear (that is, different rotation frequencies) between the shells may account for this discrepancy. In our experiment, shear could be caused by differential laser torque or the presence of impurity ions.³² For the data here, we have determined that the rotation frequency does not vary by more than 30% across the cloud. This is comparable to the limits discussed in Refs. 32 and 33.

FUTURE EXPERIMENTS

A number of future experiments will allow us to better understand strong coupling in nonneutral ion plasmas. Increasing the cooling power in the experiments should allow larger ($N_1 \gg 10^5$) samples of ions to be cooled. This may permit, perhaps by Bragg scattering,²³ the observation of structure characteristic of the infinite volume regime in which a body-centered cubic (bcc) structure is predicted.⁷ Detailed images in the Penning traps are made difficult by the rotation of the cloud which averages over azimuthal angle. In principle, it should be possible to strobe the laser (or detection) at a frequency harmonically related to ω , but this requires ω to be sufficiently stable. Fluctuations in ion density may make this difficult but perhaps an individual strongly fluorescing ion (such as Mg^+) which is locked onto the rotating lattice (of Be^+) could serve as a "beacon" and aid in determining ω . In addition, the present experiments would benefit from improved light collection optics.

At present, the rather large uncertainty in Γ in the Penning trap experiments comes from the uncertainty in our measurement of temperature. This is because the Doppler broadening contribution of the optical spectrum used is small compared to the radiative, or natural broadening. This limitation can be overcome by driving transitions whose radiative broadening is negligible as in the Hg^+ experiments.²⁴ For Be^+ and Mg^+ ions, two-photon stimulated Raman transitions might be used for this purpose.^{3,23}

So far, our measurements have been limited to the static structure of nonneutral ion plasmas. Various other experiments may provide dynamical information. For example, ions can be

switched off by optically pumping them with an additional laser beam into states which don't fluoresce.^{23,32,33} By appropriate positioning of this depopulating laser beam, certain parts of the ion cloud can be tagged allowing ion diffusion studies via the movement (or lack of movement) of the tagged ions.²⁹ In this way, relatively rapid diffusion within the shells of Be⁺ ions in the Penning trap has been distinguished from the much slower diffusion of ions between the shells. In addition, spectrum analysis of the scattered light from strongly coupled ions can possibly be used to study mode structure of ordered ion motion. Such studies may be aided by the use of sympathetic cooling³² whereby two ion species are confined simultaneously in the same trap. One ion species is laser cooled and by Coulomb interaction cools and maintains the second ion species at constant temperature. Dynamical studies are then performed on the second ion species.

It would be very useful to study large numbers of particles in a Paul trap. One clear advantage over a Penning trap is that ions can remain fixed without rotation. This could be insured by making the trap asymmetric in the x-y plane. For example, by splitting the ring into sectors and applying different static potentials to these sectors, the asymmetry could be easily controlled. For large numbers of ions, the mechanism of rf heating²⁵ must be overcome. This may be aided by working at higher laser cooling power, using smaller ratios of secular to drive frequencies (smaller q parameter, Appendix A) and making sure that impurity ions are absent.

ACKNOWLEDGEMENTS

We gratefully acknowledge support from the Office of Naval Research and the Air Force Office of Scientific Research. We thank A. Bauch for helpful suggestions on the manuscript.

APPENDIX A

In studies of strong coupling we want low temperature and high density. In addition, we may desire large numbers to more nearly approach the infinite volume regime.

Paul (rf) trap

From Eqs. 3 and 7, we can write, for a low temperature sample:

$$n_0 = 3q_r V_0 / (4\pi q \xi^2) \quad (A1)$$

where the dimensionless parameter $q_r = 4qV_0 / (m\Omega^2 \xi^2)$ is the ion's stability parameter.² Typically, $q_r < 0.3$ for stable operation. If we assume for simplicity, that U_0 is adjusted to make the cloud spherical with radius r_{c1} , the total number of ions N_i is given by

$$N_i = 4\pi n_0 r_{c1}^3 / 3 = V_0 (q_r / q) (r_{c1}^3 / \xi^2) \quad (A2)$$

Assuming q_r and r_{c1}/ξ are fixed, then to make N_i large, we want V_0 and ξ big and q small.

Similarly, we can derive

$$\Gamma = (q^5 V_0 q_r / \xi^2)^{1/3} / (k_B T), \quad (A3)$$

implying that for large Γ , we want q and V_0 big and T and ξ small. For both large N_i and Γ , we want V_0 big and T small; the choice of q and ξ may depend on specific experimental constraints.

Penning trap

If we assume a fixed value K for the ratio of the achievable density to Brillouin density and assume U_0 is chosen to make a spherical cloud (radius r_{c1}), we have

$$N_i = K B^2 r_{c1}^3 / (6mc^2), \quad (A4)$$

and

$$\Gamma = \left[\frac{K B^2}{6mc^2} \right]^{1/3} q^2 / k_B T. \quad (A5)$$

Therefore, except for practical limitations on maximum possible values of U_0 ,^{3,4} in the Penning trap, we can make both N_i and Γ large by making B , ξ ($\propto r_{c1}$), and q big and m and T small.

REFERENCES

1. J.H. Malmberg and T.M. O'Neil, Phys. Rev. Lett. 39, 1333 (1977).
2. See for example: H.G. Dehmelt, Adv. At. Mol. Phys. 3, 53 (1967) and 5, 109 (1969); D.J. Wineland, W.M. Itano, and R.S. Van Dyck, Jr., Adv. At. Mol. Phys. 19, 135 (1983).
3. See for example: D.J. Wineland and W.M. Itano, Physics Today 40(6), 34 (1987) and references therein.
4. D.J. Wineland, R.E. Drullinger, and F.L. Walls, Phys. Rev. Lett. 40, 1639 (1978). At the same time, laser cooling of ions confined in Paul (rf) trap was observed: W. Neuhauser, M. Hohenstatt, P. Toschek, and H. Dehmelt, Phys. Rev. Lett. 41, 233 (1978).
5. W. Neuhauser, M. Hohenstatt, P.E. Toschek, and H. Dehmelt, Phys. Rev. A 22, 1137 (1980).
6. W. Nagourney, Comments on At. Mol. Phys., to be published; H.G. Dehmelt, Physica Scripta, to be published.
7. S. Ichimaru, H. Iyetomi, and S. Tanaka, Phys. Rep. 149, 91 (1987) and references therein.
8. See for example: A.J. Dahm and W.F. Vinen, Physics Today 40, 43 (Feb., 1987).
9. G. Morales, these proceedings.
10. D.J. Aastuen, N.A. Clark, and L.K. Cotter, Phys. Rev. Lett. 57, 1733 (1986); J.M. di Meglio, D.A. Weitz, and P.M. Chaikin, Phys. Rev. Lett. 58, 136 (1987); C.A. Murray and D.H. Van Winkle, Phys. Rev. Lett. 58, 1200 (1987).
11. J.P. Schiffer and O. Poulsen, Europhys. Lett. 1, 55 (1986); D. Habs, in Lecture Notes in Physics 296, M. Month and S. Turner, eds. (Springer-Verlag, Berlin) 1988, p. 310.
12. J.H. Malmberg, these proceedings.
13. T.M. O'Neil, these proceedings.
14. D.J. Wineland, J.J. Bollinger, W.M. Itano, and J.D. Prestage, J. Opt. Soc. Am. B 2, 1721 (1985).
15. E. Fischer, Z. Phys. 156, 1 (1959); R.F. Wuerker, H. Shelton, and R.V. Langmuir, J. Appl. Phys. 30, 342 (1959).
16. E.C. Beaty, J. Appl. Phys. 61, 2118 (1987).
17. R.C. Davidson, Theory of Noneutral Plasmas (Benjamin, Reading, Mass., 1974), p. 7.
18. D.J. Wineland, J.C. Bergquist, W.M. Itano, J.J. Bollinger, and C.H. Manney, Phys. Rev. Lett. 59, 2935 (1987).
19. F. Diedrich, E. Peik, J.M. Chen, W. Quint, and H. Walther, Phys. Rev. Lett. 59, 2931 (1987).
20. H. Hemmati, J.C. Bergquist, and W.M. Itano, Opt. Lett. 8, 73 (1983).
21. F.G. Major and G. Werth, Appl. Phys. 15, 201 (1978); W. Neuhauser, M. Hohenstatt, P. Toschek, and H. Dehmelt, Phys. Rev. Lett. 41, 233 (1978); D.J. Wineland, J.J.

- Bollinger, and W.M. Itano, Phys. Rev. Lett. 50, 628, 1333(E) (1983).
22. W.M. Itano, et al., to be published. Our simulations agree with independent ones performed by D.H.E. Dubin (performed on up to 10 ions), private communication.
 23. J.J. Bollinger and D.J. Wineland, Phys. Rev. Lett. 53, 348 (1984); L.R. Brewer, J.D. Prestage, J.J. Bollinger, and D.J. Wineland, in Strongly Coupled Plasma Physics, edited by F.J. Rogers and H.E. Dewitt (Plenum, New York, 1987), p. 53.
 24. J.C. Bergquist, W.M. Itano, and D.J. Wineland, Phys. Rev. A36, 428 (1987).
 25. D.A. Church and H.G. Dehmelt, J. Appl. Phys. 40, 3421 (1969); H.G. Dehmelt, in Advances in Laser Spectroscopy, edited by F.T. Arecchi, F. Strumia, and H. Walther (Plenum, New York, 1983), p. 153.
 26. A. Rahman and J.P. Schiffer, Phys. Rev. Lett. 57, 1133 (1986); J.P. Schiffer, submitted for publication.
 27. H. Totsuji, in Strongly Coupled Plasma Physics, edited by F.J. Rogers and H.E. Dewitt (Plenum, New York, 1987), p. 19.
 28. D.H.E. Dubin and T.M. O'Neil, Phys. Rev. Lett. 60, 511 (1988).
 29. S.L. Gilbert, J.J. Bollinger, and D.J. Wineland, Phys. Rev. Lett., 60, 2022 (1988).
 30. J.P. Schiffer, private communication.
 31. D.H.E. Dubin, private communication.
 32. D.J. Larson, J.C. Bergquist, J.J. Bollinger, W.M. Itano, and D.J. Wineland, Phys. Rev. Lett. 57, 70 (1986).
 33. L.R. Brewer, J.D. Prestage, J.J. Bollinger, W.M. Itano, D.J. Larson, and D.J. Wineland, Phys. Rev. A., to be published.
 34. C.F. Driscoll, in Low Energy Antimatter, Ed. by D.B. Cline (World Scientific, Singapore, 1986), p. 184.